Chemosphere 215 (2019) 500–506

Contents lists available at ScienceDirect

Chemosphere

journal homepage: www.elsevier.com/locate/chemosphere

Temporal variations and potential sources of organophosphate esters in $PM_{2.5}$ in Xinxiang, North China

Kong Yang [a], Qilu Li [a, *], Meng Yuan [a], Mengran Guo [a], Yanqiang Wang [a], Shuyang Li [a], Chongguo Tian [b], Jianhui Tang [b], Jianhui Sun [a, **], Jun Li [c], Gan Zhang [c]

[a] School of Environment, Henan Normal University, Key Laboratory for Yellow River and Huai River Water Environment and Pollution Control, Ministry of Education, Henan Key Laboratory for Environmental Pollution Control, Xinxiang, Henan, 453007, PR China
[b] Key Laboratory of Coastal Environmental Processes and Ecological Remediation, Yantai Institute of Coastal Zone Research, Chinese Academy of Sciences, Yantai, 264003, China
[c] State Key Laboratory of Organic Geochemistry, Guangzhou Institute of Geochemistry, Chinese Academy of Sciences, Guangzhou, 510640, China

HIGHLIGHTS

- OPE concentrations in most samples showed slight differences at a stable level.
- Large differences of OPEs/$PM_{2.5}$ ratios in few samples may result from air mass source.
- The major source areas of OPEs and $PM_{2.5}$ were discrepant according to PSCF results.
- The major source areas of ten OPEs were diverse following PCA and PSCF results.

GRAPHICAL ABSTRACT

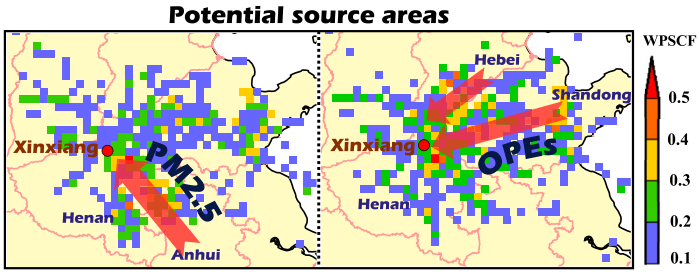

ARTICLE INFO

Article history:
Received 7 August 2018
Received in revised form
29 September 2018
Accepted 10 October 2018
Available online 10 October 2018

Handling Editor: Ebinghaus

Keywords:
Organophosphate esters
$PM_{2.5}$
Temporal variations
Potential source area
PSCF

ABSTRACT

We monitored the concentrations of 10 organophosphate esters (OPEs) in 52 fine particulate matter ($PM_{2.5}$) samples in Xinxiang, Henan Province, North China, in 2015. During the sampling period, the OPE concentrations in most samples ($n = 47$) differed minimally and were relatively stable (mean: 2.02 ± 0.93 ng m^{-3}), although several samples ($n = 5$) had high total OPE (Σ_{10}OPE) concentrations (mean: 9.99 ± 5.69 ng m^{-3}), which may have been influenced by high $PM_{2.5}$ levels. Meanwhile, some samples had high $PM_{2.5}$ concentrations but low Σ_{10}OPE concentrations (i.e. low OPE/$PM_{2.5}$ ratios) or low $PM_{2.5}$ concentrations but high Σ_{10}OPE concentrations, which might have been influenced by air mass sources. Therefore, we assessed air mass sources using the Hybrid Single Particle Lagrangian Integrated Trajectory (HYSPLIT) model and wind direction frequency data, and subsequently analysed $PM_{2.5}$ and OPE sources using a potential source contribution function (PSCF) model. The results revealed that air mass sources couldn't represent the source of specific pollutants, including $PM_{2.5}$ and OPEs. Generally, both $PM_{2.5}$ and OPEs were from Henan and Shandong Provinces; however, the major source areas differed, which may have resulted from diverse pollution characteristics in various source areas. The principal component analysis and PSCF results revealed that the 10 OPEs could be segmented into three groups, which were associated with different source areas. These results suggested that pollution characteristics of contaminants in source areas should be considered in source apportionment.

* Corresponding author.
** Corresponding author.
E-mail addresses: lqlblue@hotmail.com (Q. Li), sunjhhj@163.com (J. Sun).

https://doi.org/10.1016/j.chemosphere.2018.10.063
0045-6535/

1. Introduction

Since the restriction and banning of brominated flame retardants, organophosphate esters (OPEs) are being increasingly used worldwide as substitutes (Covaci et al., 2011; Pivnenko et al., 2017; Shaw et al., 2010). For example, the global OPE consumption in 2011 was 500,000 t, which reached 680,000 t in 2015 (Ou, 2011; van der Veen and de Boer, 2012). In China, 70,000 t of OPEs were produced in 2007, increasing to an estimated 100,000 t in 2011 (Li et al., 2015), and demand is expected to increase further by 15% annually (Deng et al., 2018; Li et al., 2015). OPEs are primarily used as additives in various industrial and commercial products, which inevitably leads to their release into the environment via volatilisation, abrasion, and dissolution (Cao et al., 2012; Regnery and Puttmann, 2010b). Therefore, OPEs have been detected in almost all environmental media, including surface water (Aznar-Alemany et al., 2018; Regnery and Puttmann, 2010a), sediment (Giulivo et al., 2017; He et al., 2017), soil (Iqbal et al., 2017; Yadav et al., 2018), air (Iqbal et al., 2017), and even human samples (Fromme et al., 2016; Xiang et al., 2017). Furthermore, several OPEs, such as tris-(2-chloroethyl) phosphate (TCEP) and tris-(1-chloro-2-propyl) phosphate (TCPP), have been found, or are suspected, to have adverse health effects (Ni et al., 2007; WHO, 1998). Given the frequent occurrence of OPEs in various samples and the study of their toxicity, OPEs have attracted considerable scientific interest.

In recent years, extensive investigations on OPEs in air including particle and gas phases, have been conducted (Möller et al., 2011; Suhring et al., 2016; Wolschke et al., 2016), but most studies have focused on OPEs in total suspended particulate matter (TSP) (Carlsson et al., 1997; Ou, 2011; Salamova et al., 2013). Fine particulate matter of aerodynamic diameter <2.5 μm ($PM_{2.5}$), has the capacity to remain for 7–30 days and can undergo long-range atmospheric transport (Yang, 2010). Therefore, $PM_{2.5}$ may carry or concentrate atmospheric OPEs during transport from urban areas to remote areas, or deposit them onto the surface of water and soil (Clark et al., 2017; Lai et al., 2015; Luo et al., 2016). The data related to OPEs in $PM_{2.5}$ are limited (Faiz et al., 2018; Liu et al., 2016; Yin et al., 2015), particularly data on the atmospheric transport of OPEs in $PM_{2.5}$. Nonetheless, existing reports indicated that OPEs may undergo long-range migration (Möller et al., 2011; Salamova et al., 2014, 2016), the OPEs pollution may be propagated via remote sources (Okonski et al., 2014), which requires more attention.

Xinxiang, Henan Province, China, is a city of along the channel of air pollution transmission to the Beijing-Tianjin-Hebei region, which experiences serious air pollution (Feng et al., 2016). For example, the mean $PM_{2.5}$ concentration in Xinxiang was 94.4 μg m^{-3} in 2015, ranking tenth among 367 cities across China (data from the China National Environmental Monitoring Centre). Moreover, the area borders Shandong Province, which is a large manufacturer of flame retardants, and Hebei Province, an area with high $PM_{2.5}$ emissions (Chen et al., 2017; Jin et al., 2008, 2010); therefore, pollution is easily distributed via ambient air masses. In this study, we collected $PM_{2.5}$ samples in Xinxiang using a high-volume sampler once weekly from Jan. to Dec. 2015. All 10 targeted OPEs were quantified to investigate their occurrence and temporal variations. Based on meteorological data, statistical analysis, and air transport model (HYSPLIT model and PSCF model), we analysed the potential source regions of $PM_{2.5}$ and OPEs.

2. Materials and methods

2.1. Sampling

The sampling campaign was conducted at Henan Normal University (35°19′29″N, 113°54′27″E) in Muye District, Xinxiang City, Henan Province, North China. The sampling site was on the roof of the School of Environment (altitude: ~100 m), which was clear of surrounding. A high-volume active sampler (Multistage Versatile Air Pollutant Sampler, $PM_{2.5}$-PUF-300, China) was deployed to collect $PM_{2.5}$ samples (n = 52) at a flow rate of 300 L min^{-1} for 24 h from Jan. 7 to Dec. 30, 2015. Detailed sampling information is presented in Table S1. All $PM_{2.5}$ samples were collected using quartz filters (Tissuquartz 2500 QAT-UP, Pallex, USA), which was calcined in a muffle furnace at 450 °C for 8 h. The filters were weighed before sampling at a temperature of 20–23 °C and relative humidity of 40 ± 1% using a Sartorius BS-124S electronic microbalance (±1 μg sensitivity; Sartorius, Göttingen, Germany). After sampling, the filters experienced freeze-drying were weighted to calculate the $PM_{2.5}$ mass. All filters were weighed in triplicate to account for errors. Then, the membrane filters were wrapped in clean aluminium foil and stored at −20 °C until chemical analysis.

2.2. Extraction

Each sample was spiked with 20 ng of deuterated surrogate standards (d_{12}-TCEP, d_{27}-TnBP, and d_{15}-TPhP). Then, the filter was extracted with 120 mL dichloromethane/n-hexane (1:1, v/v) for 36 h using Soxhlet extraction. The extract was condensed using a concentration evaporator and solvent-exchanged in n-hexane (1 mL). Next, the extract was cleaned in a silica gel column, which was packed with 4 g of silica gel (3% deactivated) and 1 g of anhydrous sodium sulphate. The F1 fraction was eluted with 20 mL of dichloromethane/n-hexane (1:1, v/v), and the F2 fraction containing OPEs was eluted with 20 mL of ethyl acetate. The F2 fraction was solvent-exchanged to n-hexane and concentrated to approximately 100 μL under a gentle nitrogen stream. Finally, 200 ng of hexamethylbenzene was added as an internal standard, and the samples were stored at −20 °C until injection.

2.3. Instrumental analysis

All 10 selected target compounds were measured in the samples: TCEP, TCPP, tri (dichloroisopropyl) phosphate (TDCPP), tri-isobutyl phosphate (TiBP), tri-n-butyl phosphate (TnBP), trihexyl phosphate (THP), tris(2-ethylhexyl) phosphate (TEHP), triphenyl phosphate (TPhP), tricresyl phosphate (TCrP), and triphenylphosphine oxide (TPPO). The samples were analysed using a gas chromatography-mass spectrometry (GC-MS) system (7890A-7010; Agilent) equipped with a programmed temperature vaporizer injector. The MS/MS system was operated in multiple reaction monitoring (MRM) mode. Meanwhile, GC separation was performed with an HP-5MS column (30 m × 0.25 mm i.d.; 0.25 μm film thickness; J&W Scientific). The MS transfer line and high-sensitivity electron impact ionisation source (HSEI) were maintained at 280 °C and 230 °C, respectively. Each sample was injected in pulsed splitless mode under the following temperature program: 50 °C for 0.2 min, 300 °C min^{-1} to 300 °C for 20 min. The GC oven temperature was as follows: 20 °C min^{-1} to 80 °C, 5 °C min^{-1} to 250 °C, 15 °C min^{-1} to 300 °C, and then held for 10 min.

2.4. Quality assurance and quality control (QA/QC)

We included a field blank and a procedural blank for every 10 samples to check for potential sample contamination. All targeted compounds were detected in field blanks (n = 5), in the range of from 0.16 ± 0.06 ng (TPPO) to 0.59 ± 0.32 ng (TCEP) (Table S2). The method detection limits (MDLs) were assigned as the average values of the field blanks plus three times the standard deviation of

the field blank values. For the present study, the average air sampling volume was 432 m^3, and the MDL were 0.77–4.34 pg m^{-3}. The recoveries of the surrogate standards were 91.3 ± 13.5% for d_{27}-TnBP, 76.3 ± 11.8% for d_{12}-TCEP, and 92.4 ± 14.3% for d_{15}-TPhP. All reported values were corrected based on the blanks and the recoveries.

2.5. Air mass back trajectories

The HYSPLIT model is a complete system developed by the National Oceanic and Atmospheric Administration (NOAA) and Australia's Bureau of Meteorology that can compute the simple air trajectories, complex dispersion, and deposition of atmospheric pollutants (Draxler and Hess, 1997). This study used 3-day (72-h) air mass back trajectories at 100 m every 3 h during each sampling period (n = 52). The trajectories during different periods were clustered to reveal the mean air mass trajectories, with the required meteorological data for the calculation obtained from the NCEP/NCAR Reanalysis Project (CDAS).

2.6. PSCF analysis

PSCF is defined as a conditional probability that an air parcel back trajectory will pass through a given site, which indicates that material from the source could be collected and transported along the trajectory to the receptor site (Pekney et al., 2006; Xie and Berkowitz, 2007). In this study, PSCF was used to assess the contribution of potential source areas to $PM_{2.5}$ and OPEs (Wang et al., 2009). The study area was segmented into grid cells, after which PSCF values were calculated for each grid cell (*i*, *j*). The equation is as follows (Jeong et al., 2011):

$$PSCF_{ij} = \frac{m_{ij}}{n_{ij}} \quad (1)$$

where n_{ij} is the total number of end points that fall in the *ij*th cell, and m_{ij} is the number of endpoints for the *ij*th cell, with arrival times at the sampling site that correspond to each type of aerosol concentration higher than an arbitrarily set criterion. Here, the 75th percentile of OPEs in $PM_{2.5}$, TCEP, TCPP, TDCPP, TiBP, TnBP, THP, TEHP, TPhP, TCrP, and TPPO (partition values: 67.2 μg m^{-3}, 0.33 ng m^{-3}, 0.19 ng m^{-3}, 0.14 ng m^{-3}, 0.06 ng m^{-3}, 0.08 ng m^{-3}, 0.045 ng m^{-3}, 0.023 ng m^{-3}, 0.055 ng m^{-3}, 0.035 ng m^{-3}, and 0.023 ng m^{-3}, respectively) were used for the PSCF calculation to identify the potential source areas.

A weighting function W (n_{ij}), applied to minimise the uncertainties caused by small n_{ij} values, was described as follows:

$$W(n_{ij}) = \begin{cases} 1.00 & n \le 80 \\ 0.75 & 20 \le n < 80 \\ 0.42 & 10 \le n < 20 \\ 0.05 & n < 10 \end{cases} \quad (2)$$

The source regions of OPEs were identified via PSCF analysis based on the 72-h backward trajectories.

2.7. Data analysis

All data were standardised before the statistical analysis to eliminate the potential influence of different units and give equal weight to each determined variable. Multiple regression, correlation analysis, and PCA were performed using SPSS software (ver. 22; IBM Corp., Armonk, NY, USA). Meanwhile, the air-mass back trajectories were determined using HYSPLIT_4, and PSCF results were performed by MeteoInfo-TrajStat. Finally, the meteorological data, including temperature, humidity, wind speed and direction, and precipitation, were obtained from the Zhenqi website (www.zq12369.com).

3. Results and discussion

3.1. Concentrations and profiles

During the sampling period, high $PM_{2.5}$ concentrations were measured in Xinxiang (mean: 94.0 ± 91.2 μg m^{-3}; range: 34.5–668 μg m^{-3}). A total of 98.1% and 50.0% of $PM_{2.5}$ levels exceeded the First Grade National Standard (35 μg m^{-3}, 24 h) and Second Grade National Standard (75 μg m^{-3}, 24 h) of China, respectively, indicative of severe $PM_{2.5}$ pollution in Xinxiang. The $\sum_{10}$OPE concentrations in $PM_{2.5}$ ranged from 0.54 ng m^{-3} to 20.0 ng m^{-3} (mean: 2.78 ± 3.00 ng m^{-3}), which were lower than the concentrations in $PM_{2.5}$ in other developed areas of China, including Nanjing (7.25 ng m^{-3}) and Chengdu (6.46 ng m^{-3}) (Faiz et al., 2018; Yin et al., 2015). The mean concentration (1.82 ± 2.45 ng m^{-3}) of three OPEs (TCEP, TCPP, and TDCPP) were much higher than those in a previous study in Xinxiang in 2014 (600 pg m^{-3}) (Liu et al., 2016), suggesting worsening OPE pollution. Among the targeted OPEs, TCEP was the most abundant component in most samples (n = 42), with a mean concentration of 1.07 ± 2.02 ng m^{-3} and range of 0.12–13.7 ng m^{-3} (Fig. 1), accounting for an average of 38.7% of $\sum_{10}$OPEs (Table S3). This was more similar to an urban site in Shanghai (37.7%) (Ren et al., 2016). TCEP was followed by TCPP (mean: 0.32 ± 0.17 ng m^{-3}; range: 0.04–0.78 ng m^{-3}) and TDCPP (mean: 0.42 ± 0.68 ng m^{-3}; range: 0.02–3.97 ng m^{-3}) (Fig. 1), which accounted for 15.3% and 14.1% of $\sum_{10}$OPEs, respectively (Table S3). The results were similar to those of a previous study (TCEP > TCPP > TDCPP) in Xinxiang (Liu et al., 2016). The other OPEs each accounted for less than 10% of $\sum_{10}$OPEs (Table S3), including TPhP (6.82%), TnBP (6.18%), TiBP (6.01%), TCrP (5.94%), TPPO (3.21%), and THP (2.93%).

3.2. Temporal variations

The overall OPE concentrations in most samples (n = 47) showed minimal variations and were stable (2.02 ± 0.93 ng m^{-3}) (Fig. 2). However, several samples had high OPE concentrations, particularly on Dec. 23 (19.9 ng m^{-3}). According to the correlation analysis, we found a significant correlation ($r = 0.85$, $P < 0.01$)

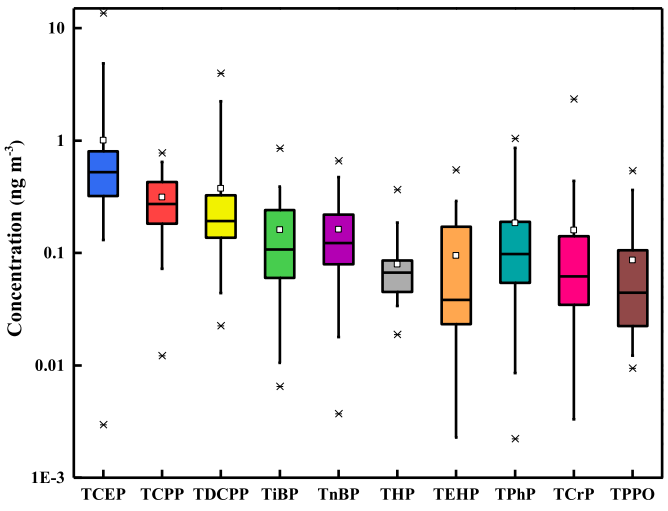

Fig. 1. The concentrations of 10 OPEs in $PM_{2.5}$ samples.

between OPE and $PM_{2.5}$ concentrations (Table S4). To reduce random errors, we further investigated the correlation between the *d*-values (i.e. differences in concentrations in two close samples) of $PM_{2.5}$ and *d*-values of OPEs, which exhibited a significant correlation ($r = 0.87$, $P < 0.01$), suggesting that high OPE concentrations were related to high $PM_{2.5}$ concentrations. In addition, the OPE profiles revealed several seasonal variations (Table S5). TCEP accounted for a significantly higher mean proportion (54%) in winter, whereas TDCPP and TCrP accounted for relatively higher proportions (26% and 14%, respectively) in summer. Since various meteorological factors ($PM_{2.5}$, temperature, humidity, and wind speed) could influence the occurrence of pollutants, we performed multiple regression of these factors associated with the concentrations of the 10 OPEs. The results indicated $PM_{2.5}$ had a significant influence on TCEP, TDCPP, THP, TEHP, TPhP, and TPPO ($r = 0.89$, 0.56, 0.51, 0.60, 0.57, and 0.72, respectively; $P < 0.01$), indicating that these OPE concentrations were likely primarily affected by $PM_{2.5}$ concentrations (Table S6). In addition, temperature was found having a significant influence on TCPP concentrations ($r = 0.37$, $P < 0.01$). Liu et al. (2016) and Li et al. (2018) found relatively higher levels in summer than in winter (Li et al., 2018; Liu et al., 2016), possibly because higher temperature promoted the release of TCPP from various products or influenced the particle/gas phase distribution. In addition, TPPO concentrations were negatively correlated with temperature, possibly the result of extremely low vapor pressure (2.6×10^{-9} Pa) and a strong association with $PM_{2.5}$ ($r = 0.72$, $P < 0.01$).

Most of OPE concentrations were significantly correlated with $PM_{2.5}$ levels; however, several samples contradicted this trend. In particular, several samples had significantly low $PM_{2.5}$ levels but high $\sum_{10}$OPE concentrations (i.e. high OPE/$PM_{2.5}$ ratios), such as those from Jan. 14 (67.3 ng g^{-1}), Jul. 1 (48.4 ng g^{-1}), and Dec. 9 (68.1 ng g^{-1}), or high $PM_{2.5}$ levels but low $\sum_{10}$OPE concentrations (i.e. low OPE/$PM_{2.5}$ ratios), such as Feb. 25 (12.3 ng g^{-1}), Oct. 15 (11.2 ng g^{-1}), and Oct.22 (13.5 ng g^{-1}) (Fig. 2). We suspected that this may have been influenced by air-mass or $PM_{2.5}$ sources; therefore, we calculated the mean mass trajectories using the HYSPLIT model for these dates. During the periods with low $PM_{2.5}$ levels but high $\sum_{10}$OPE concentrations, most of the air masses originated from northern, central, and southwestern of Henan Province, northern and central Anhui Province, south of Jiangsu Province (accounting for 71% of all trajectories), which may experience severe OPE pollution (Fig. 3a). For instance, Jiangsu Province has been reported to be a major producer of OPEs (Research of Flame Retardant Market in China). Furthermore, Henan Province is home to one of the top three plasticiser manufacturers in China (Qing'an Chemical Industry Company, capacity: 100,000 t/a, http://www.pvc123.com/b-henanqingan/). Therefore, significant emissions in these areas may have contributed to the high $\sum_{10}$OPE levels in $PM_{2.5}$ in Xinxiang. By contrast, during periods with high $PM_{2.5}$ levels but low $\sum_{10}$OPE concentrations, most of the air masses were from northwest of Xinxiang, including the Shanxi-Shaanxi-Gansu area (52%), Mongolia (15%), and southern Shandong province (33%) (Fig. 3b). These areas may have low OPE emissions due to lower production and use, resulting in lower $\sum_{10}$OPE levels in $PM_{2.5}$. Overall, the above results indicated the local sources of OPEs were stable, as most samples (n = 47) exhibited relatively small differences. Since air mass source areas could influence the OPE levels, we further analysed the external sources of OPEs.

3.3. Potential sources

3.3.1. Air mass sources

We analysed the source of air masses during the full sampling period using HYSPLIT model. The mean air mass trajectories were primarily from four directions: Hebi-Luoyang in Henan Province (35.3%), the Shanxi-Mongolia areas (26.6%), the Jiangsu Province (23.6%), and Shandong Province (14.5%), indicating that these sites may represent $PM_{2.5}$ source areas (Fig. 4). However, according to the wind direction distribution (Fig. S1a), the dominant winds originated from the east (36.5%) and northeast (25%) during the full sampling period, which differed from the HYSPLIT results. These contradictory results suggested uncertainty of air mass sources, which could be influenced by various factors such as terrain, since Xinxiang is situated south of the Taihang Mountains. Meanwhile, the air mass sources represented the source direction of air rather than sources of specific pollutants, in that the levels of pollutants in various areas were diverse. Therefore, we further analysed the potential source contribution function using the PSCF model and wind direction frequency data to clarify the $PM_{2.5}$ sources.

3.3.2. Potential source areas

According to the PSCF results for $PM_{2.5}$ (Fig. 4a), the grids of potential source contributions were in Henan Province and Shandong Province, indicating that these two provinces may be potential source areas of $PM_{2.5}$. The wind direction frequency during the heavy $PM_{2.5}$ pollution period (n = 20, Fig. S1b) revealed that the contributions of the easterly (45.0%) and southerly (S, 15.0%) winds

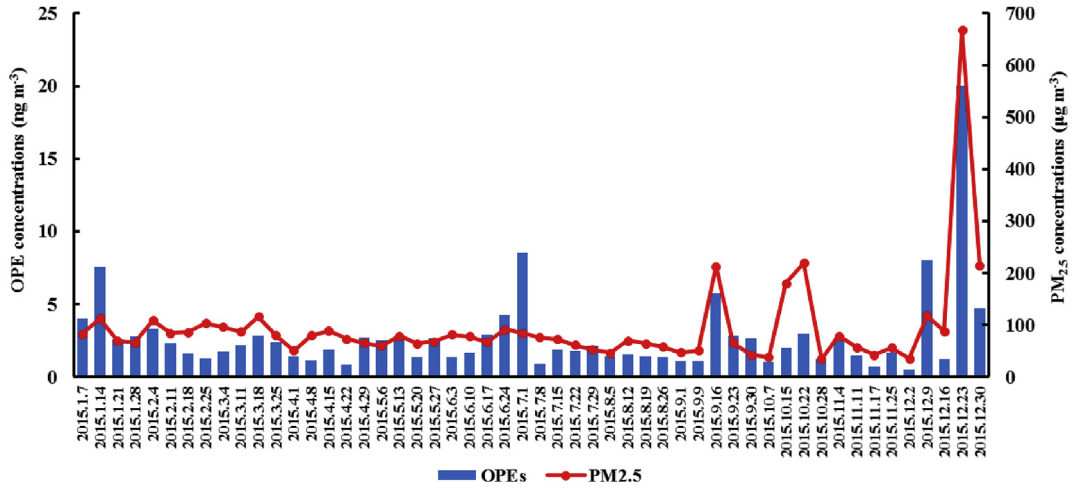

Fig. 2. The temporal variations of Σ_{10}OPEs and $PM_{2.5}$ concentrations.

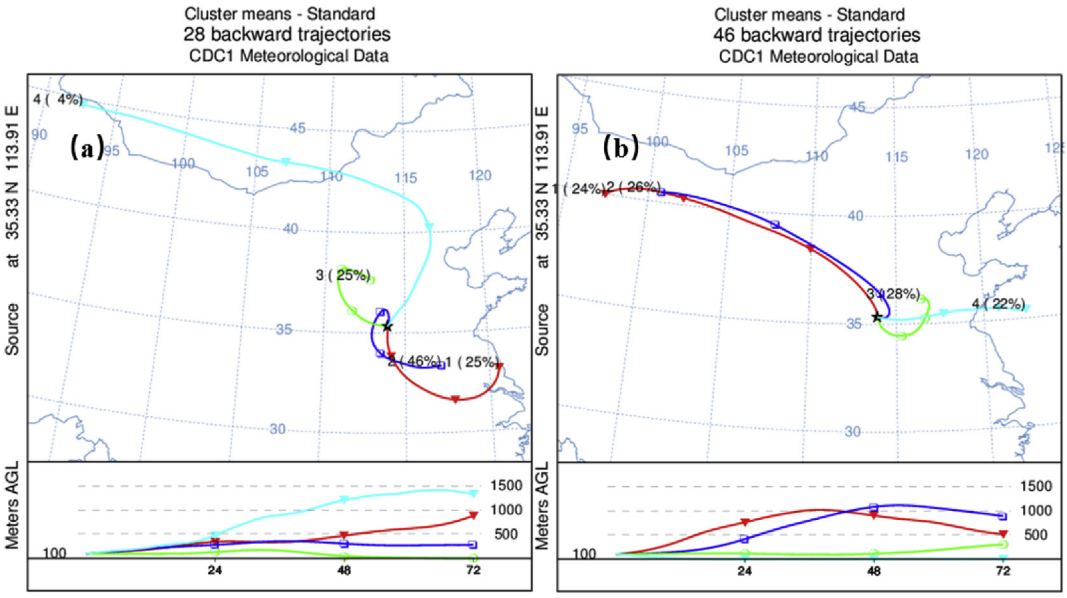

Fig. 3. The air mass back trajectories of particular samples. Note: (a) represents the sampling period had high OPEs/$PM_{2.5}$, (b) represents the sampling period had low OPEs/$PM_{2.5}$.

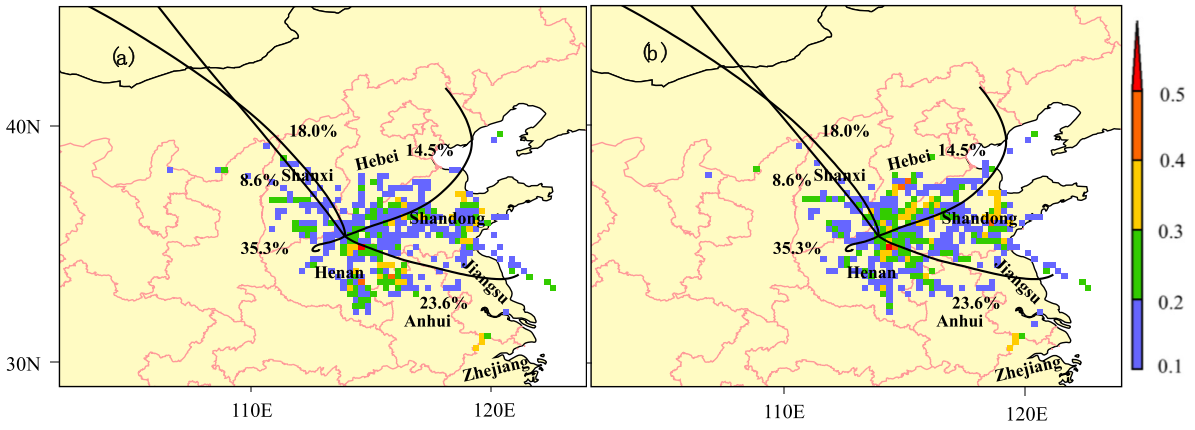

Fig. 4. The potential source areas of OPEs and $PM_{2.5}$ according to WPSCF results. Notes: (a) represents $PM_{2.5}$; (b) represents OPEs.

great during the full sampling period (east: 36.5%; south: 7.69%), indicating that the primary sources of $PM_{2.5}$ may be located to the east and south of Xinxiang. This was consistent with the PSCF results, which indicated that Shandong Province (easterly winds) and Henan Province (southerly wind) were potential source areas. Meanwhile, the contribution from the southwest (SW) is significantly higher (25%) during the slight $PM_{2.5}$ ($n = 20$) pollution period (Fig. S1c) than that during full sampling period (11.5%), indicating that this wind direction may be associated with slight $PM_{2.5}$ pollution and have a weak contribution on $PM_{2.5}$ in Xinxiang.

These results differed from the air mass source results. For instance, the primary mass trajectories (two industrial cities in Henan Province: Hebi and Luoyang) had relatively low weighted PSCF values (WPSCF) scores, indicating these areas contributed minimally to $PM_{2.5}$. This finding supported the conclusion that the air mass sources couldn't represent the origins of specific pollutants and that differences in the pollution characteristics of source areas need to be considered. Thus, we suspected that the source areas of $PM_{2.5}$ and OPEs may have differed, therefore, we analysed the potential source contribution function of OPEs during the sampling period. The results showed that the general OPE source areas were similar to those of $PM_{2.5}$ (i.e. Henan Province and Shandong Province); however, the major contribution areas exhibited. In particular, $PM_{2.5}$ (Fig. 4a) had relatively high WPSCF scores (>0.3) in central and southwest Henan Province and in northwest Anhui Province, suggesting that they may be major sources of $PM_{2.5}$. Meanwhile, OPEs (Fig. 4b) had relatively high WPSCF scores in central Henan Province, southern Hebei Province, and northwest Shandong Province, indicating these areas may be major sources of OPEs. Based on this analysis, we found several differences of sources between $PM_{2.5}$ and OPEs, thereby we speculated that the source areas of the 10 OPEs may have differed. In next section, we analysed the differences in source areas among the individual OPE congeners.

3.3.3. *Differences in OPE congeners*

We analysed the sources of the 10 OPEs and $PM_{2.5}$ using PCA. All components could be divided into three groups (Fig. 5). $PM_{2.5}$, TCEP, TPPO, TEHP, and TPhP had high scores under PC1 (42.9%), TDCPP, TCrP, and THP had high scores under PC2 (18.1%), and TCPP, TnBP,

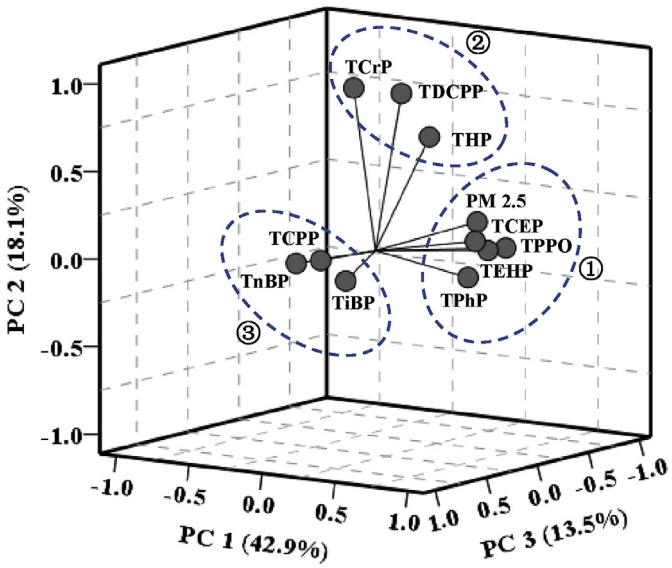

Fig. 5. The principle component analysis of 10 OPEs and $PM_{2.5}$.

and TiBP have high scores under PC3 (13.5%). Components with close scores indicated that they may have been derived from similar sources. By contrast, the OPEs grouped in PC1, PC2, and PC3 may have originated different sources.

Based on these results, we explored the potential source areas of the 10 OPEs using a PSCF model. The overall potential source areas of all 10 OPEs were consistent with those of $PM_{2.5}$, primarily including Shandong Province and Henan Province (Figs. S2, S3, and S4). However, the major contribution areas showed several variations among the groups and patterns within a given group. For the first group (Fig. S2), the potential source areas of TCEP, TEHP, and TPhP were similar to those of $PM_{2.5}$ (Fig. 4a), consistent with the PCA results, indicating they may have originated from the same sources. Meanwhile, TPPO had significantly high WPSCF scores (>0.2) in a large area, mainly over Shandong Province (Fig. S2), differing from the other components. In the second group, relatively high WPSCF values (0.2–0.5) were found in southeast and northeast Xinxiang, particularly for TDCPP and TCrP (Fig. S3). The results concurred with the higher PC2 scores of TDCPP and TCrP, indicating that OPEs may have originated from these two directions. Finally, the components of the third group (Fig. S4) had high WPSCF values around the border of Shandong Province bounded by Henan, Anhui, and Jiangsu Provinces, which differed in their potential $PM_{2.5}$ source areas, indicating these areas may be the primary sources of TCPP, TnBP, and TiBP. The consistency of PCA and PSCF results indicated OPEs congeners in the same group might be from similar sources.

4. Conclusion

In this study, we measured the concentrations of 10 targeted OPEs in $PM_{2.5}$ in Xinxiang, North China. The results (mean Σ_{10}OPE concentration: $2.78 \pm 3.00\ ng\ m^{-3}$) revealed lower than those in developed areas in China, such as Nanjing ($7.25\ ng\ m^{-3}$) and Chengdu ($6.46\ ng\ m^{-3}$). In addition, the Σ_{10}OPE concentrations displayed only slight temporal variations (mean: $2.02 \pm 0.93\ ng\ m^{-3}$, $n = 47$), excluding several dates with high concentrations, which may have been influenced by high $PM_{2.5}$ levels. Further, we observed several samples with highly varying OPE/$PM_{2.5}$ ratios, which, according to the HYSPLIT results, may have been influenced by different air mass source areas. To further clarify this, we analysed the source areas of air masses, $PM_{2.5}$, and OPEs based on the HYSPLIT model, PSCF model, and wind frequency data. The results of the sources of air mass, $PM_{2.5}$, and OPEs exhibited several differences, revealing that air masses may not represent the actual pollutant sources. The PCA and PSCF results of the 10 OPEs showed that they could be divided into three groups sharing similar sources: TCEP, TEHP, TPhP, and TPPO; TDCPP, TCrP, and THP; and TCPP, TiBP, and TnBP. These results highlight the importance of using a combination of methods and pollution characteristics when analysing the sources of atmospheric pollutants.

Acknowledge

This work was supported by Postdoctoral Science Foundation of China (2016M600581), the National Natural Science Foundation of China (41703126), National Key R&D Program of China (2017YFC0212000), and Key Project of Science and Technology in Henan Province (152102310316).

Appendix A. Supplementary data

Supplementary data to this article can be found online at https://doi.org/10.1016/j.chemosphere.2018.10.063.

References

Aznar-Alemany, O., Aminot, Y., Vila-Cano, J., Kock-Schulmeyer, M., Readman, J.W., Marques, A., Godinho, L., Botteon, E., Ferrari, F., Boti, V., Albanis, T., Eljarrat, E., Barcelo, D., 2018. Halogenated and organophosphorus flame retardants in European aquaculture samples. Sci. Total Environ. 612, 492–500.

Cao, S., Zeng, X., Song, H., Li, H., Yu, Z., Sheng, G., Fu, J., 2012. Levels and distributions of organophosphate flame retardants and plasticizers in sediment from Taihu Lake, China. Environ. Toxicol. Chem. 31 (7), 1478–1484.

Carlsson, H., Nilsson, U., Becker, G., Östman, C., 1997. Organophosphate ester flame retardants and plasticizers in the indoor environment: Analytical methodology and occurrence. Environ. Sci. Technol. 31 (10), 2931–2936.

Chen, Z., Cai, J., Gao, B., Xu, B., Dai, S., He, B., Xie, X., 2017. Detecting the causality influence of individual meteorological factors on local $PM_{2.5}$ concentration in the Jing–Jin–Ji region. Sci. Rep. 7, 40735.

Clark, A.E., Yoon, S., Sheesley, R.J., Usenko, S., 2017. Spatial and temporal distributions of organophosphate ester concentrations from atmospheric particulate matter samples collected across Houston, TX. Environ. Sci. Technol. 51 (8), 4239–4247.

Covaci, A., Harrad, S., Abdallah, M.A., Ali, N., Law, R.J., Herzke, D., de Wit, C.A., 2011. Novel brominated flame retardants: a review of their analysis, environmental fate and behaviour. Environ. Int. 37 (2), 532–556.

Deng, W.J., Li, N., Wu, R., Richard, W.K.S., Wang, Z., Ho, W., 2018. Phosphorus flame retardants and Bisphenol A in indoor dust and $PM_{2.5}$ in kindergartens and primary schools in Hong Kong. Environ. Pollut. 235, 365–371.

Draxler, R.R., Hess, G.D., 1997. Description of HYSPLIT_4 Modeling Systerm. NOAA Technical Memorandum ERL ARL–224.

Faiz, Y., Siddique, N., He, H., Sun, C., Waheed, S., 2018. Occurrence and profile of organophosphorus compounds in fine and coarse particulate matter from two urban areas of China and Pakistan. Environ. Pollut. 233, 26–34.

Feng, J., Yu, H., Su, X., Liu, S., Li, Y., Pan, Y., Sun, J.H., 2016. Chemical composition and source apportionment of $PM_{2.5}$ during Chinese Spring Festival at Xinxiang, a heavily polluted city in North China: fireworks and health risks. Atmos. Res. 182, 176–188.

Fromme, H., Becher, G., Hilger, B., Volkel, W., 2016. Brominated flame retardants – exposure and risk assessment for the general population. Int. J. Hyg Environ. Health 219 (1), 1–23.

Giulivo, M., Capri, E., Kalogianni, E., Milacic, R., Majone, B., Ferrari, F., Eljarrat, E., Barcelo, D., 2017. Occurrence of halogenated and organophosphate flame retardants in sediment and fish samples from three European river basins. Sci. Total Environ. 586, 782–791.

He, H., Gao, Z., Zhu, D., Guo, J., Yang, S., Li, S., Zhang, L., Sun, C., 2017. Assessing bioaccessibility and bioavailability of chlorinated organophosphorus flame retardants in sediments. Chemosphere 189, 239–246.

Iqbal, M., Syed, J.H., Breivik, K., Chaudhry, M.J.I., Li, J., Zhang, G., Malik, R.N., 2017. E-waste driven pollution in Pakistan: the first evidence of environmental and human exposure to flame retardants (FRs) in Karachi City. Environ. Sci. Technol. 51 (23), 13895–13905.

Jeong, U., Kim, J., Lee, H., Jung, J., Kim, Y.J., Song, C.H., Koo, J.H., 2011. Estimation of the contributions of long range transported aerosol in East Asia to carbonaceous aerosol and PM concentrations in Seoul, Korea using highly time resolved measurements: a PSCF model approach. J. Environ. Monit. 13 (7), 1905–1918.

Jin, J., Liu, W., Wang, Y., Yan Tang, X., 2008. Levels and distribution of

polybrominated diphenyl ethers in plant, shellfish and sediment samples from Laizhou Bay in China. Chemosphere 71 (6), 1043–1050.
Jin, J., Wang, Y., Yang, C., Hu, J., Liu, W., Cui, J., 2010. Human exposure to polybrominated diphenyl ethers at production area, China. Environ. Toxicol. Chem. 29 (5), 1031–1035.
Lai, S., Xie, Z., Song, T., Tang, J., Zhang, Y., Mi, W., Peng, J., Zhao, Y., Zou, S., Ebinghaus, R., 2015. Occurrence and dry deposition of organophosphate esters in atmospheric particles over the northern South China Sea. Chemosphere 127, 195–200.
Li, J., Tang, J., Mi, W., Tian, C., Emeis, K.C., Ebinghaus, R., Xie, Z., 2018. Spatial distribution and seasonal variation of organophosphate esters in air above the Bohai and Yellow Seas, China. Environ. Sci. Technol. 52 (1), 89–97.
Li, P., Li, Q.X., Ma, Y.L., Jin, J., Wang, Y., Tian, Y., 2015. Determination of organophosphate esters in human serum using gel permeation chromatograph and solid phase extraction coupled with gas chromatography–mass spectrometry. Chin. J. Anal. Chem. 43 (7), 1033–1039.
Liu, D., Lin, T., Shen, K., Li, J., Yu, Z., Zhang, G., 2016. Occurrence and concentrations of halogenated flame retardants in the atmospheric fine particles in Chinese cities. Environ. Sci. Technol. 50 (18), 9846–9854.
Luo, P., Bao, L.J., Guo, Y., Li, S.M., Zeng, E.Y., 2016. Size-dependent atmospheric deposition and inhalation exposure of particle-bound organophosphate flame retardants. J. Hazard Mater. 301, 504–511.
Möller, A., Xie, Z., Caba, A., Sturm, R., Ebinghaus, R., 2011. Organophosphorus flame retardants and plasticizers in the atmosphere of the North Sea. Environ. Pollut. 159 (12), 3660–3665.
Ni, Y., Kumagai, K., Yanagisawa, Y., 2007. Measuring emissions of organophosphate flame retardants using a passive flux sampler. Atmos. Environ. 41 (15), 3235–3240.
Okonski, K., Degrendele, C., Melymuk, L., Landlova, L., Kukucka, P., Vojta, S., Kohoutek, J., Cupr, P., Klanova, J., 2014. Particle size distribution of halogenated flame retardants and implications for atmospheric deposition and transport. Environ. Sci. Technol. 48 (24), 14426–14434.
Ou, Y., 2011. Developments of Organic Phosphorus Flame Retardant Industry in China.
Pekney, N.J., Davidson, C.I., Zhou, L., Hopke, P.K., 2006. Application of PSCF and CPF to PMF–modeled sources of $PM_{2.5}$in Pittsburgh. Aerosol Sci. Technol. 40 (10), 952–961.
Pivnenko, K., Granby, K., Eriksson, E., Astrup, T.F., 2017. Recycling of plastic waste: screening for brominated flame retardants (BFRs). Waste Manag. 69, 101–109.
Regnery, J., Puttmann, W., 2010a. Occurrence and fate of organophosphorus flame retardants and plasticizers in urban and remote surface waters in Germany. Water Res. 44 (14), 4097–4104.
Regnery, J., Puttmann, W., 2010b. Seasonal fluctuations of organophosphate concentrations in precipitation and storm water runoff. Chemosphere 78 (8), 958–964.
Ren, G., Chen, Z., Feng, J., Ji, W., Zhang, J., Zheng, K., Yu, Z., Zeng, X., 2016. Organophosphate esters in total suspended particulates of an urban city in East China. Chemosphere 164, 75–83.
Salamova, A., Hermanson, M.H., Hites, R.A., 2014. Organophosphate and halogenated flame retardants in atmospheric particles from a European Arctic site. Environ. Sci. Technol. 48 (11), 6133–6140.
Salamova, A., Ma, Y., Venier, M., Hites, R.A., 2013. High levels of organophosphate flame retardants in the great lakes atmosphere. Environ. Sci. Technol. Lett. 1 (1), 8–14.
Salamova, A., Peverly, A.A., Venier, M., Hites, R.A., 2016. Spatial and temporal trends of particle phase organophosphate ester concentrations in the atmosphere of the Great Lakes. Environ. Sci. Technol. 50 (24), 13249–13255.
Shaw, S.D., Blum, A., Weber, R., Kannan, K., Rich, D., Lucas, D., Koshland, C.P., Dobraca, D., Hanson, S., Birnbaum, L.S., 2010. Halogenated flame retardants: do the fire safety benefits justify the risks? Rev. Environ. Health 25 (4), 261–305.
Suhring, R., Wolschke, H., Diamond, M.L., Jantunen, L.M., Scheringer, M., 2016. Distribution of organophosphate esters between the gas and particle phase-model predictions vs measured data. Environ. Sci. Technol. 50 (13), 6644–6651.
van der Veen, I., de Boer, J., 2012. Phosphorus flame retardants: properties, production, environmental occurrence, toxicity and analysis. Chemosphere 88 (10), 1119–1153.
Wang, Y.Q., Zhang, X.Y., Draxler, R.R., 2009. TrajStat: GIS–based software that uses various trajectory statistical analysis methods to identify potential sources from long–term air pollution measurement data. Environ. Model. Software 24 (8), 938–939.
WHO, 1998. EHC 209: Flame Retardants: Tris-(Chloropropyl)Phosphate and Tris-(2-chloroethyl)phosphate, Geneva, Switzerland.
Wolschke, H., Sühring, R., Mi, W., Möller, A., Xie, Z., Ebinghaus, R., 2016. Atmospheric occurrence and fate of organophosphorus flame retardants and plasticizer at the German coast. Atmos. Environ. 137, 1–5.
Xiang, P., Liu, R.Y., Li, C., Gao, P., Cui, X.Y., Ma, L.Q., 2017. Effects of organophosphorus flame retardant TDCPP on normal human corneal epithelial cells: implications for human health. Environ. Pollut. 230, 22–30.
Xie, Y., Berkowitz, C.M., 2007. The use of conditional probability functions and potential source contribution functions to identify source regions and advection pathways of hydrocarbon emissions in Houston, Texas. Atmos. Environ. 41 (28), 5831–5847.
Yadav, I.C., Devi, N.L., Li, J., Zhang, G., 2018. Organophosphate ester flame retardants in Nepalese soil: spatial distribution, source apportionment and air-soil exchange assessment. Chemosphere 190, 114–123.
Yang, T., 2010. Chemical Compositions and Source Apportionment of $PM_{2.5}$ in Changsha. Central South University, Changsha (in China).
Yin, H., Li, S., Ye, Z., Yang, Y., Liang, J., You, J., 2015. Pollution level and source of organic phosphorus esters in airborne $PM_{2.5}$ in Chengdu city. China. Environ. Sci. 36 (10), 3566–3572.